

## Improvement of the signal-to-noise ratio of laser-induced-fluorescence photon-counting signals of single-atoms magneto-optical trap

This article has been downloaded from IOPscience. Please scroll down to see the full text article.

2011 J. Phys. D: Appl. Phys. 44 135102

(<http://iopscience.iop.org/0022-3727/44/13/135102>)

View [the table of contents for this issue](#), or go to the [journal homepage](#) for more

Download details:

IP Address: 218.26.243.164

The article was downloaded on 11/03/2011 at 02:14

Please note that [terms and conditions apply](#).

# Improvement of the signal-to-noise ratio of laser-induced-fluorescence photon-counting signals of single-atoms magneto-optical trap

Jun He, Baodong Yang, Tiancai Zhang and Junmin Wang<sup>1</sup>

State Key Laboratory of Quantum Optics and Quantum Optics Devices, and Institute of Opto-Electronics, Shanxi University, No. 92 Wucheng Road, Taiyuan 030006, Shanxi Province, People's Republic of China

E-mail: [wjjmm@sxu.edu.cn](mailto:wjjmm@sxu.edu.cn)

Received 16 October 2010, in final form 21 January 2011

Published 10 March 2011

Online at [stacks.iop.org/JPhysD/44/135102](http://stacks.iop.org/JPhysD/44/135102)

## Abstract

Employing grating extended-cavity diode lasers as the cooling/trapping and repumping lasers for preparing and manipulating single atoms, we have implemented a large-magnetic-gradient caesium magneto-optical trap (MOT). To detect and evaluate single caesium atoms trapped in MOT, laser-induced-fluorescence (LIF) photons of trapped atoms driven by MOT lasers are collected and counted by an avalanched photodiode worked in photon-counting mode. The dependences of LIF photon-counting signals of single atoms on a cooling laser's intensity, frequency detuning and frequency fluctuation are analysed and investigated. Remarkable improvement of the signal-to-noise ratio of LIF photon-counting signals is achieved by optimizing the cooling laser's intensity and frequency detuning and using the modulation-free polarization spectroscopic technique with feedback to both the slow channel (piezoelectric transducer channel with typical bandwidth of  $\sim 2$  kHz in the grating extended cavity) and the fast channel (current modulation channel with typical bandwidth of  $\sim 200$  kHz in the current driver).

(Some figures in this article are in colour only in the electronic version)

## 1. Introduction

The interaction of atoms with light has been an important theme in investigations of behaviour of the microscopic world. Typically, a variety of fundamental investigations require a sample consisting of an individual atom that is spatially localized with small kinetic energy. Single atoms in a magneto-optical trap (MOT) [1–9] or in an optical dipole trap [5, 10–14] are very significant to demonstrate and perform quantum information processing. Several applications, such as quantum register [10], triggered single-photon source [11], atom-photon entanglement [12] and coherent manipulation of atomic qubit [13, 14] have been demonstrated. Quite often, the detection schemes of these experiments employ a near-resonance laser beam that drives a cycling atomic transition

and a high numerical aperture lens assembly to collect the light-induced-fluorescence (LIF) photons of trapped atoms to a photomultiplier tube (PMT) or an avalanche photodiode (APD). For single atoms, the fluorescence signal is so weak that it is strongly restrained by the intensity and fluctuation of scattering rate and the accuracy of manipulation. Many of the experiments rely on the ability not only to trap and manipulate atoms but also to collect and distinguish weak fluorescence signals.

The signal-to-noise ratio (SNR) of LIF photon-counting signals of single atoms is crucial. In the process of atoms interacting with laser beams, the magnitude and fluctuation of signals depend on the fluctuation of the intensity and frequency of exciting laser. When one makes the improvement in LIF photon-counting signals, in addition to enhancing the signal magnitude, better frequency stabilization techniques

<sup>1</sup> Author to whom any correspondence should be addressed.

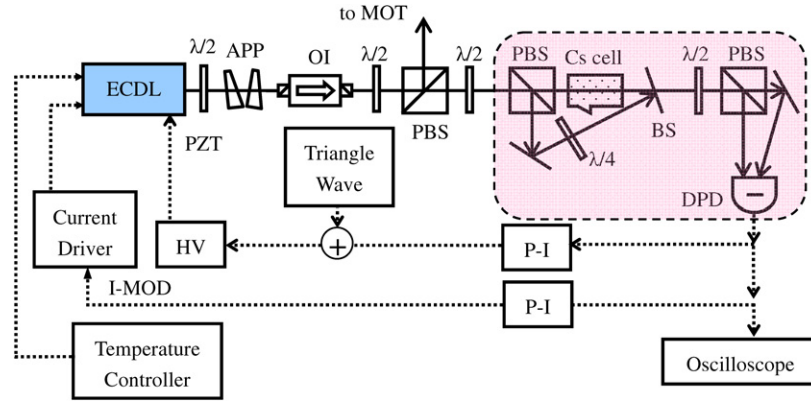


**Figure 1.** The schematic diagram of experimental setup for frequency locking by modulation-free PS scheme. ECDL: grating extended-cavity diode laser;  $\lambda/2$ : half-wave plate;  $\lambda/4$ : quarter-wave plate; APP: anamorphic prisms pair; OI: optical isolator; PBS: polarization beam splitter cube; BS: 50/50 beam splitter plate; DPD: differential photodiode; PI: proportion-and-integration amplifier; HV: high voltage amplifier; I MOD: current modulation channel in the current driver (the fast channel); PZT: piezoelectric transducer in the extended cavity (the slow channel). The part in the dashed-line frame is the polarization spectrometer. The solid arrow lines indicate optical path and the dotted arrow lines are for electronic connection.

should be required to restrain the LIF signal fluctuation. Various techniques of laser frequency stabilization have been demonstrated. Usually transition frequency of atoms is adopted as frequency standard for frequency stabilization. In one popular method, saturation absorption spectroscopy (SAS) is widely employed to lock the laser frequency. Laser frequency modulation and phase-sensitive detection (PSD) are normally used to generate a dispersion-like frequency discriminating signal for frequency correcting [15]. Direct frequency modulation in the SAS scheme unavoidably generates extra noise in laser frequency and intensity. Alternatively, modulation-free frequency stabilization has been demonstrated by several kinds of techniques: the Zeeman shift induced dichroism of atomic transition [16–18], acousto-optical modulators (AOM) shift induced dichroism of atomic transition [19–21] and the polarization spectroscopy (PS) [22, 23]. In particular, the PS scheme can be implemented simply and inexpensively, and also can acquire a preferable SNR of dispersion-like signal, so it has been applied to stabilize the frequency of dye lasers and diode lasers for years [24–27].

For demonstration of coherent manipulation of single caesium atom as well as triggered single-photon source based on the single atom, we cool and trap a single caesium atom in a large-magnetic-gradient MOT and detect the single atoms by counting LIF photons driven by cooling transition [4, 5]. In our experiment, the cooling/trapping and repumping beams of MOT are provided by grating extended-cavity diode lasers (ECDLs). The laser frequency fluctuation will be transferred into the scattering rate fluctuation of trapped atoms, which leads to extra noises of LIF photon-counting signals. Active frequency stabilization to the stable reference is required in our experiment. Here we perform modulation-free PS in a caesium vapour cell to obtain a dispersion-like signal, and lock ECDLs (to caesium  $6S_{1/2}F_g = 4-6P_{3/2}F_e = 5$  hyperfine transition for the cooling/trapping laser and to  $6S_{1/2}F_g = 3-6P_{3/2}F_e = 4$  hyperfine transition for the repumping laser) via feedbacks to both of the slow channel (piezoelectric transducer (PZT) channel with bandwidth of  $\sim 2$  kHz in the grating extended-cavity) and the fast channel (current modulation channel with

bandwidth of  $\sim 200$  kHz in the current driver) to depress the frequency drifting and jitter. Compared with the conventional frequency-modulation SAS lock scheme, the modulation-free PS lock scheme with feedback to both of the slow and fast channels can achieve relatively better frequency stability, thus yielding clear improvement of LIF photon-counting signal of single trapped atoms.

This paper is organized as follows: in section 2, we describe the experimental setup of realizing the frequency stabilization by the modulation-free PS locking scheme. Then we present the ECDL frequency stabilization results and relevant discussion; in section 3, first we discuss the SNR of single atoms based on the scattering theory and give the results of simulation for typical parameters. Then we compare the experimental results for the application of the SAS modulation lock scheme usually used and the modulation-free PS lock scheme in our single-atoms MOT. After that we quote the major quantitative results for comparison with the results of other groups, and give an explanation. Finally, a conclusion is given.

## 2. ECDL frequency stabilization

The experimental setup of laser frequency stabilization is shown in figure 1 schematically. Here we only show frequency stabilization of the ECDL for MOT cooling/trapping laser. The ECDL for MOT repumping laser is similar except locking to the caesium  $6S_{1/2}F_g = 3-6P_{3/2}F_e = 4$  hyperfine transition. A home-made 852 nm grating ECDL with the Littrow configuration is used to provide the cooling/trapping beams for our single caesium atoms MOT [4, 5]. Typical output power is 40 mW after passing through the anamorphic prisms pair (APP, for beam shaping) and the 40 dB optical isolator (OI). The laser frequency can be scanned continuously over  $\sim 3$  GHz without mode hopping by adopting a triangle-wave voltage to the slow channel.

The main part of output power used for MOT is picked up by a combination of a half-wave plate ( $\lambda/2$ ) and a polarization

beam splitter (PBS) cube. A weak linearly polarized beam ( $\sim 3$  mW) is used for PS, as illustrated in the dashed-line frame in figure 1. The laser beam is separated into two parts by a combination of  $\lambda/2$  plate and PBS. The weak transmission beam used as the probe beam is sent through a 30 mm long caesium vapour cell with a diameter of 20 mm, while the strong reflection beam used as the pump beam is steered by a mirror and is converted from linear polarization to circular polarization by a quarter-wave plate ( $\lambda/4$ ), and then partially reflected by a beam-splitting (BS) plate to counter-propagate along the probe beam to pass through the caesium cell. The diameter of the pump beam ( $\sim 110$   $\mu$ W) and the probe beam ( $\sim 30$   $\mu$ W) is  $\sim 3$  mm. The probe beam finally is separated into two parts by a combination of  $\lambda/2$  plate and PBS, and detected by a differential photodiode (DPD). This balanced detection method is slightly different from the conventional PS scheme [22, 23] in which the probe beam passed through the sample placed between two crossed polarizers is detected. Here, the balanced detection can eliminate background and improve the SNR of PS signal.

Caesium atoms in ground states are uniformly populated at the different Zeeman sub-levels without pump beam. While the circularly polarized pump beam passes through the caesium cell, population in Zeeman sub-levels of ground state is no longer uniform because of the different Clebsch–Gordan coefficients. This non-uniform population on the Zeeman sub-levels will make atomic vapour anisotropy [22, 23]. The linearly polarized probe beam can be decomposed into two counter-rotating circularly polarized ingredients. Induced anisotropy will lead to the difference in the absorption and refractive index for each of the two ingredients of the probe beam. This yields a dispersion-like PS signal from the DPD detector without frequency modulation, and it can serve as frequency discriminating signal for laser frequency stabilization. This point is very important for frequency stabilization because this modulation-free scheme can avoid adding extra noise to laser frequency and intensity, and better frequency stability would be expected. Figure 2 shows typical PS signal with the dispersion-like profiles for the caesium  $6S_{1/2}F_g = 4-6P_{3/2}F_e = 3, 4$  and 5 transitions. For comparison and frequency calibration SAS signal recorded with the same sweep range is also shown in figure 2. In particular, because of the strongest transition strength, the dispersion-like PS signal corresponding to the  $6S_{1/2}F_g = 4-6P_{3/2}F_e = 5$  cycling transition has the largest amplitude. Under the optimum condition, the slope of the zero-crossing point in the dispersion-like signal is about  $1.47$  MHz  $V^{-1}$ , and SNR is about 22. The polarity of the dispersion signal can be understood by a simple picture [26]. For the  $F_g = 4-F_e = 5$  closed transition, the population is optically pumped into the  $|F_g = 4, m_F = +4\rangle$  state (or  $|F_g = 4, m_F = -4\rangle$  state, depends on the pump beam's polarization; here we consider  $\sigma^+$ -polarized pump beam). According to the Clebsch–Gordan coefficients, the line strength of the  $\sigma^+$  transition from the  $|F_g = 4, m_F = +4\rangle$  state is significantly larger than the  $\sigma^-$  transition. For the  $F_g = 4-F_e = 4$  transition, the  $|F_g = 4, m_F = +4\rangle$  state has no electronic excited state for the  $\sigma^+$  transition. Therefore only the  $\sigma^-$  component of the probe beam interacts with the

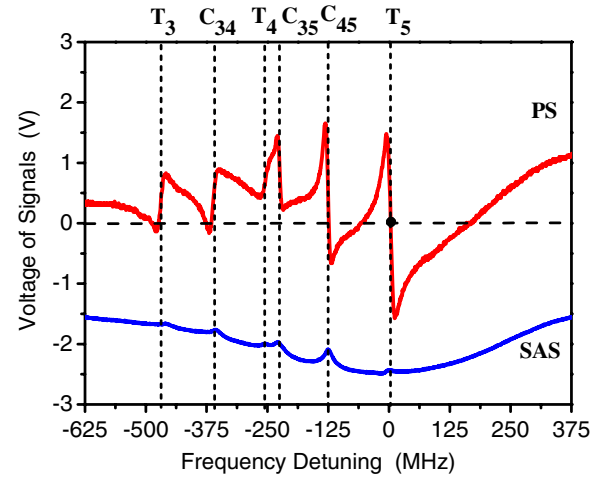


**Figure 2.** Typical polarization spectra (PS) of caesium  $6S_{1/2}F_g = 4-6P_{3/2}F_e = 3, 4$  and 5 hyperfine transitions and crossover lines. Saturation absorption spectrum (SAS) is shown for frequency calibration.  $T_5$  ( $F_g = 4-F_e = 5$  cycling transition) is reasonably selected as zero detuning.  $T_3$  denotes the  $F_g = 4-F_e = 3$  hyperfine transition, and  $T_4$  denotes the  $F_g = 4-F_e = 4$  transition.  $C_{34}$  ( $F_g = 4-F_e = 3$  and 4),  $C_{35}$  ( $F_g = 4-F_e = 3$  and 5) and  $C_{45}$  ( $F_g = 4-F_e = 4$  and 5) are the crossover lines, respectively. The solid circle is the point of reference for realizing the frequency stabilization, which needs to be offset to zero value in experiment.

atoms. Consequently, the polarity of the dispersion signal has the opposite sign relative to the  $F_g = 4-F_e = 5$  transition. For the  $F_g = 4-F_e = 3$  transition, the signal inversion compared with the  $F_g = 4-F_e = 5$  transition also occurs owing to the same reason.

For close-loop locking, the error-correcting signal is amplified for feedbacks to both the slow channel and the fast channel to depress the frequency drifting and jitter. The PZT moves the blazing grating in ECDL to keep the laser at the reference frequency, and reduces the frequency drifting induced by acoustic noise, residual temperature fluctuation and laser current fluctuation. However, if we only use the slow channel (PZT channel), it has a very limited bandwidth (DC  $\sim 2$  kHz). Here the fast channel (current channel) with broader bandwidth (DC  $\sim 200$  kHz) is also employed in our experiment. Figure 3 shows the frequency error signals within 200 s for the case of ECDL free running and after being locked with feedback to both of the slow and fast channels with the modulation-free PS lock scheme. Typical frequency fluctuations of  $\sim 12$  MHz for the free-running case and less than  $\pm 100$  kHz after being locked are estimated. It is very clear that the frequency drifting and jitter are restrained by the active stabilization.

### 3. Dependence of LIF photon-counting signals of single-atoms MOT on experimental parameters

A schematic diagram of our single-atom MOT is depicted in figure 4. A cuboid glass cell with optical quality and anti-reflection coating on surface is evacuated by a vacuum pump system (not shown) to keep the pressure between  $1 \times 10^{-10}$  and  $2 \times 10^{-11}$  Torr with caesium atoms released from the atomic reservoir. The two groups of cooling/trapping beams

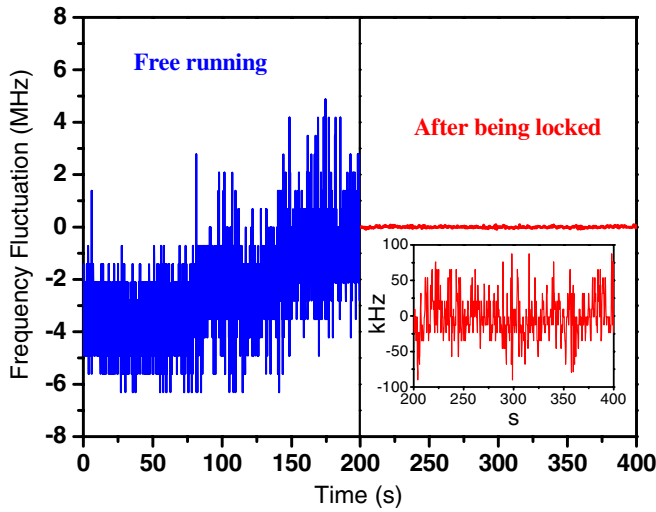


**Figure 3.** Frequency error signals for the free-running case and the locked case. In the free-running case, typical frequency fluctuation is  $\sim 12$  MHz in 200 s. In the locked case, ECDL is stabilized by the modulation-free PS scheme with feedback to both of the slow and fast channels; the residual frequency fluctuation is less than  $\pm 100$  kHz in 200 s.

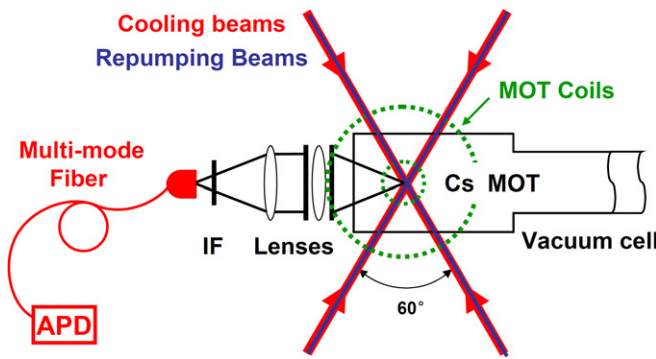


**Figure 4.** Schematic diagram of single-atoms magneto-optical trap (MOT). The dotted circle indicates the position of anti-Helmholtz magnetic coils for MOT. Cs: caesium atoms; IF: interference filter @ 852 nm; APD: avalanche photodiode.

in the horizontal plane which intersect with an angle of  $60^\circ$  are indicated, and the other one group of cooling/trapping beams perpendicular to the horizontal plane is not shown in figure 4. The dotted circles show anti-Helmholtz magnetic coils which are mounted above and beneath the glass cell. We determine the exact number of trapped atoms by efficiently collecting and detecting LIF photons from trapped atoms driven by cooling transition. The fluorescence collecting lens assembly is mounted outside the glass cell and has a numerical aperture of 0.29. A fibre-coupled APD worked in photon-counting mode is used for counting LIF photons of trapped atoms.

To obtain good SNR, on the one hand, we need to increase the signal intensity; on the other hand, we must restrain the fluctuation of fluorescence signal. Large signal intensity with a small fluctuation can narrow the distribution of LIF photons and be very helpful to distinguish the changes between each step for judging the number of atoms in MOT accurately. In the part below, we will explain how the laser frequency and intensity affect the photon scattering rate. Here we adopt a

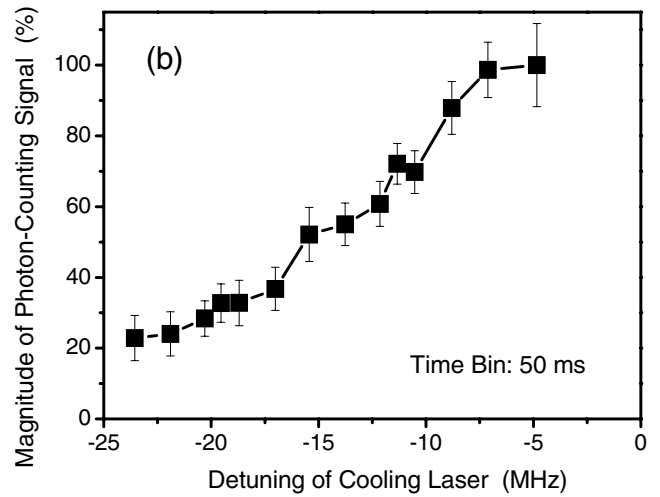
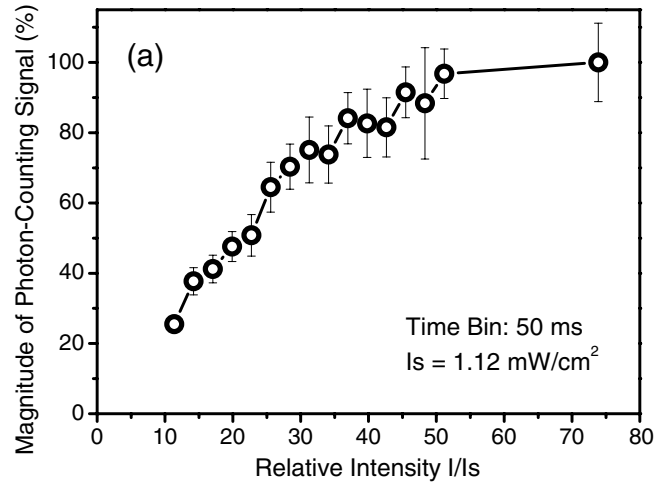


**Figure 5.** Magnitude of LIF photon-counting signals of single atom trapped in MOT versus the relative intensity of cooling laser  $I/I_s$  (a) and the frequency detuning of cooling laser (b). The circles and solid squares are experimental data, while the solid lines are just for guiding eyes. The error bars are given in terms of statistical standard deviation.

simple model to analyse this process, which gives an option to optimize experimental parameters. The photon scattering rate  $R_{sc}$  of atoms can be depicted as follows [28]:

$$R_{sc} = \frac{\Gamma}{2} \cdot \frac{I/I_s}{1 + I/I_s + 4(\Delta/\Gamma)^2}, \quad (1)$$

where  $\Gamma = 2\pi \times 5.22$  MHz is the spontaneous decay rate for the caesium  $6P_{3/2}F_e = 5-6S_{1/2}F_g = 4$  hyperfine transition,  $\Delta$  is the angular frequency detuning of excitation laser (cooling/trapping laser),  $I$  is the total laser intensity of excitation laser (cooling/trapping laser) and  $I_s$  is the saturation intensity for the  $F_g = 4-F_e = 5$  transition. The scattering rate depends on the intensity and detuning of cooling laser beams. Figure 5 shows the dependence of LIF photon-counting signal on cooling/trapping laser's parameters. The data are taken with a single atom in the MOT. Increasing the laser intensity and decreasing the red detuning of cooling/trapping laser can enhance the signal magnitude.

According to equation (1), fluctuations of laser intensity and frequency can be transferred into the scattering rate

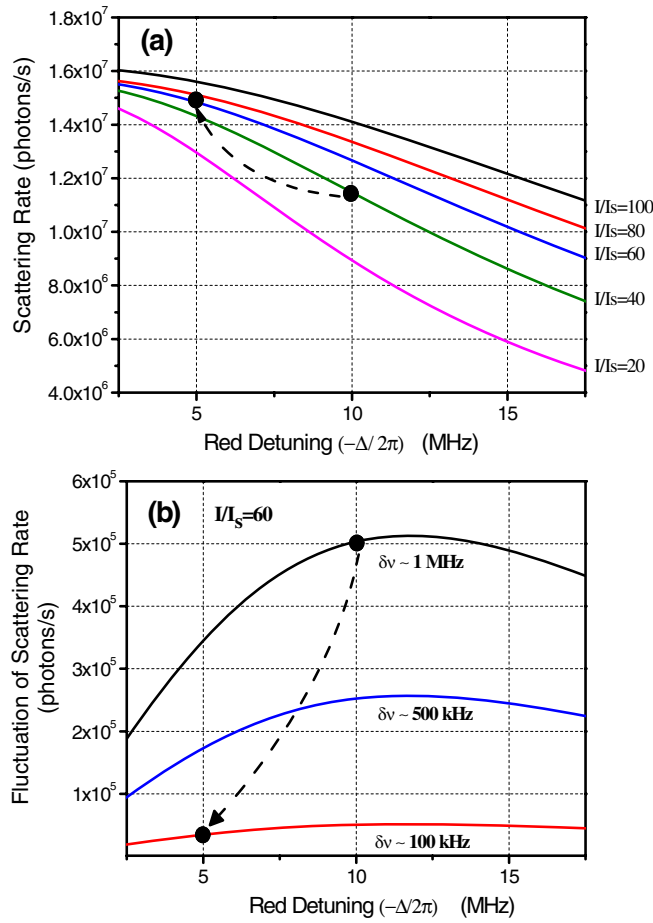


**Figure 6.** Simulation results. (a) Photon scattering rate of single atom in MOT versus the red detuning of cooling/trapping laser with parameter of the laser intensity ( $I/I_s$ ). (b) Fluctuation of photon scattering rate of single atom in MOT versus the red detuning of cooling/trapping laser with parameter of the frequency fluctuation of cooling/trapping laser ( $\delta\nu$ ). The solid circles and the dash lines with arrow indicate the experimental parameters of our single-atoms MOT before and after optimization.

fluctuation and make the SNR of LIF photon-counting signal blurred. Simulations have been performed for the case of a single atom trapped in MOT and the results are shown in figure 6. Suppression of residual frequency fluctuation of cooling/trapping laser can clearly improve the SNR of LIF photon-counting signal (figure 6(b)). For improving the SNR, total laser intensity of cooling and trapping beams is changed from  $\sim 40I_s$  to  $\sim 60I_s$  (see figure 6(a)), and frequency detuning  $\Delta/2\pi$  to the  $F_g = 4 - F_e = 5$  transition is changed from  $\sim (-10)$  MHz to  $\sim (-5)$  MHz. We stabilized the ECDL system using the modulation-free PS lock scheme, instead of the SAS modulation lock scheme used in [4]. The residual frequency fluctuation after locking is decreased to  $\sim \pm 100$  kHz (see figure 3). The scattering rate fluctuation of a single caesium atom in MOT decreasing from  $\sim 5.0 \times 10^5$  to  $\sim 3.4 \times 10^4$  photons  $s^{-1}$  will be expected after all these improvements. Under roughly the same conditions of the background pressure, laser intensity and frequency detuning, we compared the typical discrete LIF photon-counting signals of an individual trapped caesium atom for cases of the

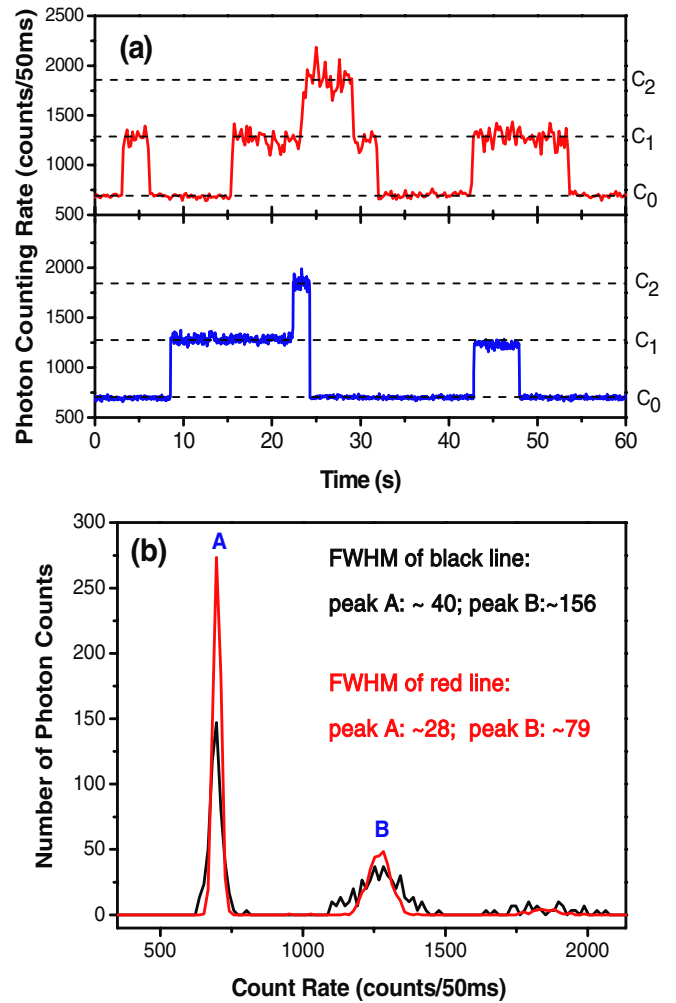


**Figure 7.** (a) Well separated discrete fluorescence photon-counting levels.  $C_0$ ,  $C_1$  and  $C_2$  indicate the photon-counting rate levels in time bin of 50 ms for no atom (due to the stray light from the cooling/trapping lasers of the empty trap), one atom, and two atoms in MOT, respectively. The upper trace indicates photon-counting signal for the case of ECDL's frequency stabilized by the frequency-modulation SAS lock scheme, while the lower trace indicates that for the case of ECDL's frequency stabilized by the modulation-free PS lock scheme with feedback to both of the slow and fast channels. (b) Histogram of the photon-counting data. Signal-to-noise ratio is remarkably improved.

frequency-modulation SAS lock scheme and the modulation-free PS lock scheme, as shown in figure 7. The photon-counting rate for the background counts is  $\sim 700$  in the time bin of 50 ms. For different frequency stabilization schemes, the  $C_0$  is approximately the same under the same experimental parameters. The photon-counting rate levels of  $C_1$  and  $C_2$  is dominated by the laser intensity and frequency detuning. The scattering theory suggests that there is a sensitive dependence of fluctuation of  $C_1$  and  $C_2$  on the laser frequency jitter and drifting as well as laser intensity noise. Direct frequency modulation of cooling/trapping laser in the SAS scheme will unavoidably add extra noise into the laser frequency and the laser intensity. The frequency stabilization by the modulation-free PS lock scheme with feedbacks to both the slow and fast channels can effectively restrain the frequency jitter and

drifting, thus the fluctuation of the LIF photon-counting signal can be suppressed effectively.

Here we discuss the experimental results for the SNR in some detail and compare our experimental results with the data of other groups:

- (1) The background photon-counting is caused by scattering photons of the whole system entering the APD, which should be as small as possible in experiment. The power stability of laser and the system stability are the key parameters for the background photon-counting fluctuation. As shown in figure 7(a) and (b), our results show that the FWHM (full width at half maximum) of background photon-counting distribution is reduced from  $\sim 40$  to  $\sim 28$  after the adoption of the optimized modulation-free PS lock scheme with other unchanged parameters, which is dominated by laser intensity noise under the same system condition;
- (2) The fluctuation of scattering rate depends on the fluctuation of laser intensity and frequency. Figure 7(b) shows the distribution of the frequency occurrence of the LIF photon-counting arising from change in scattering rate. After adopting the optimized modulation-free PS lock scheme, the FWHM of scattering rate distribution of single-atom signal is reduced from  $\sim 156$  to  $\sim 79$ , which is mainly limited by residual laser frequency fluctuation. We also present the LIF photon-counting signals in the time bin of 200 ms, with FWHM background photon-counting of  $\sim 88$  and FWHM of scattering rate distribution for single atom  $\sim 198$ . We found that our recent results agree with the theoretical analysis qualitatively;
- (3) The time bin of data acquisition card for photon counting is about several tens of ms or 100 ms, which should be much shorter than the lifetime of trapped atoms (several tens of seconds in our case) and much longer than the spontaneous lifetime ( $\sim 30.5$  ns for the caesium  $F_e = 5 - F_g = 4$  transition) [29]. The magnitude and fluctuation of signal are related to the time bin of data acquisition card. Different time bin shows a different average effect of data in different time scales. The time bin for data shown in figure 7 is 50 ms, which means that the output is a summation of the photon counting every 50 ms. If longer time bin is adopted, the average time for accumulation will be longer, thus the signal is intensified and the fluctuation of noise will be smoothed. We have studied the dependence of fluctuation of the signal on the time bin for comparison with the average effect and a list of different time scales is given in table 1. When the time bin is 200 ms, under the normal condition the fluctuation of signal and the background photon-counting are the smallest under the same detuning and intensity of laser;
- (4) We also quote the major quantitative experiments results for comparison with other groups. The SNR is  $\sim 4.9$  in our results (as shown in table 1) when we set the time bin to 100 ms, which is clearly better compared with the results demonstrated by other groups (the relevant results from others groups are estimated and listed in table 2) under the certain condition of 100 ms time bin. We need to emphasize that one must be cautious in

quantitative comparison because the absolute value of the laser intensity and frequency detuning are different.

To improve the SNR of LIF photon-counting signals of trapped atoms, this paper has presented an effective solution, and it has been clearly demonstrated by experimental data. The significance and possible application of improvement of the SNR are stated as below. Firstly, in actual single-atom trap experiments, since the LIF signal from the trapped atom is extremely weak, one needs to choose a time bin for photon counting as long as possible in order to achieve better SNR. However, in order to prepare and examine the quantum state of the single atom, one needs to control laser beams, identify and detect the LIF signal of the atoms in the trap in the time scale of millisecond or even microsecond, which leads to increase in signal fluctuation. Meanwhile, the signal intensity output by data record card decreases with the same proportion as time bin decreases, and the step-like signal may be totally submerged due to the fluctuation of signal. Therefore, high SNR is the primary condition. Secondly, when demonstrating the initialization, readout and fast manipulation of qubits stored in a string of single atoms, the laser intensity and frequency fluctuation will lead to the fluctuation of Rabi frequency, thus the preparation of quantum coherence superposition states will be influenced, which demands optimization of the laser system. The SNR of the LIF photon-counting signals of single atom in this work is much better than our previous results [4] and also clearly better than most other groups' results (see tables 1 and 2). The validity of analysis was confirmed by comparing our results with other groups', which is helpful for optimizing the experiments. Moreover, this improvement may allow us to use single atom as a sensitive probe of quantum dynamics, and it can be easily extended to the case of the cold atoms trapped in optical tweezer, in which one can employ LIF photon-counting signal to determine the exact number of trapped atoms and to identify the hyperfine state the trapped atoms populated (state-selective detection).

#### 4. Conclusion

In conclusion, more stable locking of ECDLs to the caesium hyperfine transition is achieved by employing modulation-free PS with feedbacks to both the slow and fast channels of ECDLs. The experimental results for the SNR of the LIF photon-counting signal of single trapped atoms are presented and the noticeable progress we have made in experiment is discussed, which is attributed to better frequency stability of the cooling/trapping laser. Explanation of the LIF photon-counting signals from single atoms is shown, which allow us to quantitatively discuss the results for comparison with other groups. Analysis of the magnitude and fluctuation of signal is shown. Measurements of the LIF photon-counting signals are found to be in agreement with the analysis, at least qualitatively. The much better SNR of the LIF photon-counting signals of single atom provides us with a very good starting point for further manipulation of the single atom using MOT and optical tweezer. Obviously, in other cases in which if higher frequency stability of ECDL is required, the modulation-free PS lock scheme with feedbacks to both the slow and fast channels would be a simple and very helpful solution.

**Table 1.** The dependence of fluctuation of the signal on time bin.

	Time bin (ms)	Background counts	Fluctuation of background counts	Signals for single atom	Fluctuation of atomic signals	SNR
Our Results	50	~700	~74	~571	~175	~3.3
	100	~1399	~112	~1143	~232	~4.9
	200	~2799	~152	~2312	~343	~6.7

**Table 2.** Estimations of quantitative results in references about the signal intensity and noise.

Ref.	Time bin (ms)	Background counts	Fluctuation of background counts	Signals of single atom	Fluctuation of atomic signals	SNR
[30]	100	~2000	~300	~2300	~1445	~1.6
[33]	100	~40	~34	~180	~85	~2.1
[35]	100	~8700	~1849	~5100	~2000	~2.6
[31]	20	~10	~16	~50	~40	~1.3
[32]	200	~627	~261	~653	~346	~1.9
[34]	10	~21	~28	~39	~40	~1.0
[36]	100	~3500	~1160	~9500	~3000	~3.2

## Acknowledgments

This work was partially supported by the National Natural Science Foundation of China (Grant Nos 60978017, 61078051 and 10974125), the Project for Excellent Research Team of the National Natural Science Foundation of China (Grant No 60821004) and the NCET Program from the Education Ministry of China (Grant No NCET-07-0524). Authors thank Miss Jing Wang for her contributions to this experiment in the earlier stage.

## References

- [1] Hu Z and Kimble H J 1994 Observation of a single atom in a magneto-optical trap *Opt. Lett.* **19** 1888
- [2] Haubrich D, Schadwinkel H, Strauch F, Ueberholz B, Wynands R and Meschede D 1996 Observation of individual neutral atoms in magnetic and magneto-optical traps *Europhys. Lett.* **34** 663
- [3] Ruschewitz F, Bettermann D, Peng J L and Ertmer W 1996 Statistical investigations on single trapped neutral atoms *Europhys. Lett.* **34** 651
- [4] Wang J, He J, Qiu Y, Yang B D, Zhao J Y, Zhang T C and Wang J M 2008 Observation of single neutral atoms in a large-magnetic-gradient vapour-cell magneto-optical trap *Chin. Phys. B* **17** 2062
- [5] He J, Wang J, Yang B D, Zhang T C and Wang J M 2009 Single atoms transferring between a magneto-optical trap and a far-off-resonance optical dipole trap *Chin. Phys. B* **18** 3404
- [6] Chen C Y, Li Y M, Bailey K, O'Connor T P, Young L and Lu Z T 1999 Ultrasensitive isotope trace analyses with a magneto-optical trap *Science* **286** 1139
- [7] Hoekstra S, Mollema A K, Morgenstern R, Wilschut H W and Hoekstra R 2005 Single-atom detection of calcium isotopes by atom-trap trace analysis *Phys. Rev. A* **71** 023409
- [8] Hill S B and McClelland J J 2003 Atoms on demand: fast, deterministic production of single Cr atoms *Appl. Phys. Lett.* **82** 3128
- [9] Yoon S, Choi Y, Park S, Kim J, Lee J H and An K 2006 Definitive number of atoms on demand: controlling the number of atoms in a few-atom magneto-optical trap *Appl. Phys. Lett.* **88** 211104
- [10] Schrader D, Dotsenko I, Khudaverdyan M, Miroshnychenko Y, Rauschenbeutel A and Meschede D 2004 Neutral atom quantum register *Phys. Rev. Lett.* **93** 150501
- [11] Darquie B, Jones M P A, Dingjan J, Beugnon J, Bergamini S, Sortais Y, Messin G, Browaeys A and Grangier P 2005 Controlled single-photon emission from a single trapped two-level atom *Science* **309** 454
- [12] Volz J, Weber M, Schlenk D, Rosenfeld W, Vrana J, Saucke K, Kurtsiefer C and Weinfurter H 2006 Observation of entanglement of a single photon with a trapped atom *Phys. Rev. Lett.* **96** 030404
- [13] Yavuz D D, Kulatunga P B, Urban E, Johnson T A, Proite N, Henage T, Walker T G and Saffman M 2006 Fast ground state manipulation of neutral atoms in microscopic optical traps *Phys. Rev. Lett.* **96** 063001
- [14] Jones M P A, Beugnon J, Gaetan A, Zhang J, Messin G, Browaeys A and Grangier P 2007 Fast quantum state control of a single trapped neutral atom *Phys. Rev. A* **75** 040301
- [15] Ikegami T, Sudo S and Sakai Y 2000 *Frequency Stabilization of Semiconductor Laser Diodes* (Boston, MA: Atech House)
- [16] Corwin K L, Lu Z T, Hand C F, Epstein R J and Wieman C E 1998 Frequency-stabilized Diode laser with the Zeeman shift in an atomic vapor *Appl. Opt.* **37** 3295
- [17] Beverini N, Maccioni E, Marsili P, Ruffini A and Sorrentino F 2001 Frequency stabilization of a diode laser on the Cs D<sub>2</sub> resonance line by the Zeeman effect in a vapor cell *Appl. Phys. B* **73** 133
- [18] Wang J M, Yan S B, Wang Y H, Liu T and Zhang T C 2004 Modulation-free frequency stabilization of a grating-external-cavity diode laser by magnetically-induced sub-Doppler dichroism in cesium vapor cell *Japan. J. Appl. Phys.* **43** 1168
- [19] Madej A A, Marmet L and Bernard J E 1998 Rb atomic absorption line reference for single Sr<sup>+</sup> laser cooling systems *Appl. Phys. B* **67** 229
- [20] Sukenik C I, Busch H C and Shiddiq M 2002 Modulation-free laser frequency stabilization and detuning *Opt. Commun.* **203** 133
- [21] van Ooijen E D, Katgert G and van der Straten P 2004 Laser frequency stabilization using Doppler-free bichromatic spectroscopy *Appl. Phys. B* **79** 57
- [22] Wieman C and Hänsch T W 1976 Doppler-free laser polarization spectroscopy *Phys. Rev. Lett.* **36** 1170
- [23] Harris M L, Adams C S, Cornish S L, McLeod I C, Tarleton E and Hughes I G 2006 Polarization

- spectroscopy in rubidium and cesium *Phys. Rev. A* **73** 062509
- [24] Kim J B, Kong H J and Lee S S 1988 Dye laser frequency locking to the hyperfine structure ( $3S_{1/2}$   $F = 2$ – $3P_{1/2}$   $F = 2$ ) of sodium  $D_1$  line by using polarization spectroscopy *Appl. Phys. Lett.* **52** 417
- [25] Kozuma M, Kourogi M, Ohtsu M and Hori H 1992 Frequency stabilization, linewidth reduction, and fine detuning of a semiconductor laser by using velocity-selective optical pumping of atomic resonance line *Appl. Phys. Lett.* **61** 1895
- [26] Yoshikawa Y, Umeki T, Mukae T, Torii Y and Kuga T 2003 Frequency stabilization of a laser diode with use of light-induced birefringence in an atomic vapor *Appl. Opt.* **42** 6645
- [27] Borisov P A, Melentiev P N, Rudnev S N and Balykin V I 2005 Simple system for active frequency stabilization of a diode laser in an external cavity *Laser Phys.* **15** 1523
- [28] Foot C J 2005 *Atomic Physics* (Oxford: Clarendon) p 180
- [29] Kang S, Yoon S, Choi Y, Lee J H and An K 2006 Dependence of fluorescence-level statistics on bin-time size in a few-atom magneto-optical trap *Phys. Rev. A* **74** 013409
- [30] Zuo Z, Fukusen M, Tamaki Y, Watanabe T, Nakagawa Y and Nakagawa K 2009 Single atom Rydberg excitation in a small dipole trap *Opt. Express* **17** 22898
- [31] He X D, Xu P, Wang J and Zhan M S 2009 Rotating single atoms in a ring lattice generated by a spatial light modulator *Opt. Express* **17** 21017
- [32] Choi Y, Yoon S, Kang S, Kim W, Lee J H and An K 2007 Direct measurement of loading and loss rates in a magneto-optical trap with atom-number feedback *Phys. Rev. A* **76** 013402
- [33] Weber M, Volz J, Saucke K, Kurtsiefer C and Weinfurter H 2006 Analysis of a single-atom dipole trap *Phys. Rev. A* **73** 043406
- [34] Schlosser N, Reymond G, Protsenko I and Grangier P 2001 Sub-poissonian loading of single atoms in a microscopic dipole trap *Nature* **411** 1024
- [35] Frese D, Ueberholz B, Kuhr S, Alt W, Schrader D, Gomer V and Meschede D 2000 Single atoms in an optical dipole trap: towards a deterministic source of cold atoms *Phys. Rev. Lett.* **85** 3777
- [36] Gomer V, Ueberholz B, Knappe S, Strauch F, Frese D and Meschede D 1998 Decoding the dynamics of a single trapped atom from photon correlations *Appl. Phys. B* **67** 689